INTERNATIONAL JOURNAL OF CLIMATOLOGY
Int. J. Climatol. **26**: 723–741 (2006)
Published online 26 January 2006 in Wiley InterScience (www.interscience.wiley.com). DOI: 10.1002/joc.1277

SYNOPTIC CLIMATOLOGICAL INFLUENCES ON THE SPATIAL AND TEMPORAL VARIABILITY OF AEROSOLS OVER NORTH AMERICA

HELEN C. POWER,[a,*] SCOTT C. SHERIDAN[b] and JASON C. SENKBEIL[b]
[a] *Department of Geography, University of Otago, Dunedin, New Zealand*
[b] *Department of Geography, Kent State University, Kent, Ohio, USA*

Received 3 June 2005
Revised 31 August 2005
Accepted 15 September 2005

ABSTRACT

The spatial and temporal variability of atmospheric aerosols is not well understood, as most studies have been constrained to data sets that include few stations and are of short duration. Furthermore, all methods for quantifying atmospheric turbidity suffer from a major constraint in that they require cloudless sky conditions. This restriction produces gaps in the turbidity record and sampling bias, which has led to questionable inferences about the variability of aerosols.

In this research, we address these concerns via analyses at scales broader than all previous studies. We analyzed the spectral aerosol optical depth at 500 nm (τ_{a5}) and Ångström's wavelength exponent (α), which represents the relative size distribution of aerosols. A total of 27 sites, with a mean period of record of 7.3 years, are included. Beyond seasonal and spatial summaries of aerosol variability, we have divided observations by synoptic condition, utilizing the Spatial Synoptic Classification (SSC).

Our results show that atmospheric turbidity across North America is greatest over the east. Seasonality of both parameters was shown, most notably a greater τ_{a5} during summertime. Utilizing the SSC, we have uncovered significant differences across weather types. Moist weather types, especially moist tropical, display considerably higher turbidity, while the colder, drier dry polar weather type is associated with low aerosol optical depth. Certain weather types show considerable seasonal variability; the dry tropical weather type is associated with relatively low values in winter, but high values in summer, when convection is significant. Cluster analyses of stations yielded three general regions, each with similar synoptic variability: a western cluster with low aerosol optical depth and minimal synoptic variability, an eastern cluster with higher turbidity and variability, and a cluster located on the periphery of the eastern cluster, associated with moderate levels of turbidity but very high variability, suggesting a varied influence of nearby industrial areas. Copyright © 2006 Royal Meteorological Society.

KEY WORDS: aerosols; climate variability; synoptic climatology; atmospheric turbidity

1. INTRODUCTION

Aerosols play an important role in the energy balance of the Earth–atmosphere system. Despite their importance, the interaction between aerosols and climate is still a source of great uncertainty in understanding climate and climate change (Lohmann *et al*., 2000; Ghan *et al*., 2001; IPCC, 2001; Anderson *et al*., 2003a). Part of the uncertainty is because aerosols typically demonstrate large spatial and temporal variability, variability that has not been well documented. Perhaps equally important, the mechanisms that determine this variability are not fully understood (Penner *et al*., 2001; Anderson *et al*., 2003b).

A reciprocal relationship exists between aerosols and climate: while aerosols affect radiative exchanges, climate and meteorology have a profound influence on temporal and spatial patterns in atmospheric turbidity (defined as the total amount of aerosol integrated through the vertical atmospheric column). At the microscale, for example, higher humidity can enhance hygroscopic aerosol growth (Pilinis *et al*., 1995; Kotchenruther

* Correspondence to: Helen C. Power, Department of Geography, University of Otago, Dunedin, New Zealand;
e-mail: hcp@geography.otago.ac.nz

et al., 1999; Kay and Box, 2000; Smirnov *et al*., 2000; Holben *et al*., 2001; Ramaswamy *et al*., 2001), while higher insolation may also enhance photochemical conversion of gases to aerosols (Peterson and Flowers, 1977; Holben *et al*., 2001). At the mesoscale, the stability of the atmosphere and convective processes can influence the amount of aerosol in the atmosphere (e.g. Al-Jamal *et al*., 1987; Kambezidis *et al*., 1998; Augustine *et al*., 2003). On an even larger scale, turbidity is influenced by the origin, trajectory, and travel time of the synoptic air mass (Peterson *et al*., 1981; Smirnov *et al*., 1994, 1995, 1996, 2000; Jacovides *et al*., 1996; Pinker *et al*., 1997; Kambezidis *et al*., 1998).

A number of studies have evaluated the role of climate and meteorology in aerosol variability over North America. Previous studies include Flowers *et al*. (1969), Peterson *et al*. (1981), Halthore *et al*. (1992), Smirnov *et al*. (1994, 1996, 2000), Wenny *et al*. (1998), Yu *et al*., (2000, 2001), Holben *et al*. (2001), Im *et al*. (2001a, 2001b), Ingold *et al*. (2001), and Augustine *et al*. (2003). Collectively, these authors evaluated aerosol data together with surface weather maps, upper-level charts, meteorological observations, back trajectory analyses, and rawinsonde data. They attributed spatial and temporal trends in turbidity to spatial and temporal differences in insolation, humidity, temperature, wind speed, precipitation events, rates of convection, and the source regions and types of air masses. These physical parameters influence the production, type, growth, size, residence time, and transport of aerosols.

These studies were limited in their geographic extent, the extent of their meteorological or climatological analyses, and/or the duration and quality of aerosol data evaluated. Flowers *et al*. (1969), for example, evaluated turbidity data from multiple sites across the United States, but these data are now more than 30 years old and were derived from less reliable handheld single-wavelength sunphotometers. Wenny *et al*. (1998), Yu *et al*. (2000, 2001), and Im *et al*. (2001a, 2001b) evaluated aerosol data and air mass origin in North Carolina, but their data included only two sites with durations of only 3 and 7 months respectively. Smirnov *et al*. (2000) used aerosol data from six stations in the United States; however, the time series were only for 1 month and they were restricted to coastal and island locations in New Jersey, Maryland, and Virginia. Of the remaining studies, the maximum number of sites evaluated in North America was five (Holben *et al*., 2001).

In addition to these limitations, all aerosol studies suffer from a temporal constraint in that existing methods for quantifying atmospheric turbidity require cloudless sky conditions. This clear-sky restriction produces gaps in the turbidity record. Since clear-sky conditions are associated with certain synoptic conditions, such undersampling means that aerosol climatologies may contain a bias and, therefore, may not be truly representative.

In this research, we have performed a thorough analysis of the variability in aerosols across North America by evaluating coincident aerosol and meteorological data from 27 monitoring stations in the United States and Canada, all of which include at least 3 years of data. Meteorological data are incorporated into this work via a weather-type classification system, which also helps identify the synoptic conditions most oversampled and undersampled within existing aerosol climatologies.

2. BACKGROUND

Two optical properties of aerosols are evaluated in this research: the spectral (wavelength-specific) aerosol optical depth τ_a, which provides a dimensionless measure of the total column amount of aerosol, and Ångström's wavelength exponent (α), which describes the wavelength dependence of τ_a and is a dimensionless measure of the aerosol size distribution. Theoretically, the value of α can range from 4, for a high ratio of small to large particles, to less than 0 for a low ratio of small to large particles, although typical values are usually between 0.5 and 2.5. Ångström's wavelength exponent gives an indication of the origin or type of aerosol. Aerosols of maritime, desert, crustal, or volcanic origin, for example, are relatively large and are associated with smaller values of α (von Hoyningen-Huene *et al*., 1999; Chiapello *et al*., 2000; Maring *et al*., 2000; Smirnov *et al*., 2000; Holben *et al*., 2001). Aerosols from biomass burning or anthropogenic sources (e.g. industrial or vehicular emissions), in contrast, are typically relatively small and are thus represented by higher values of α (e.g. Deuzé *et al*., 2001; Eck *et al*., 2001; Formenti *et al*., 2001; Holben *et al*., 2001).

The spectral aerosol optical depth is the vertical integral of the ambient aerosol extinction coefficient. To determine τ_a, the total optical depth is calculated from the spectral extinction of direct beam radiation on the basis of the Beer–Bouguer Law. Attenuation due to Rayleigh scatter and absorption by ozone and gaseous pollutants are estimated and removed to isolate the aerosol optical depth. Ångström's wavelength exponent is calculated from Ångström's equation (Ångström, 1929, 1930):

$$\tau_{a\lambda} = \beta\lambda^{-\alpha} \tag{1}$$

where $\tau_{a\lambda}$ is the aerosol optical depth at wavelength λ and β is the aerosol optical depth at a wavelength of 1.0 μm. The value of α is computed as the slope of the linear regression of $\ln \tau_{a\lambda}$ *versus* $\ln \lambda$.

More recently, satellite observations have been used to quantify aerosol optical properties (e.g. Deuzé *et al*., 2001; Zhang *et al*., 2001; Knapp *et al*., 2002). Although satellite estimates of turbidity can provide greater spatial coverage than surface-based (point) measurements, comparisons of collocated satellite and surface measurements have shown biases in the satellite estimates especially over terrestrial regions (e.g. Higurashi *et al*., 2000; Deuzé *et al*., 2001; Haywood *et al*., 2001; Zhang *et al*., 2001). This is, in part, because satellite estimates are subject to subpixel inhomogeneity of aerosol properties as well as cloud contamination (Hsu *et al*., 1999). Thus, reliable measurements of aerosol optical properties rely on surface-based observations.

Historically, surface-based aerosol monitoring has been sporadic, short-term, and limited in scope geographically (Holben *et al*., 2001). However, during the last decade, systematic surface-based aerosol-monitoring programs have emerged. For example, in 1993, the National Aeronautics and Space Administration (NASA) initiated a comprehensive surface-based aerosol-monitoring program known as the Aerosol Robotic Network (AERONET). This program is supported by international, national and local agencies, individuals, universities, and private foundations worldwide (Holben *et al*., 1998, 2001). Close to 200 identical automatic Cimel spectral radiometers are currently deployed throughout the world, including North America. This network provides the most accurate and comprehensive long-term measurement of aerosol optical properties available (Holben *et al*., 1998, 2001; Dubovik *et al*., 2000; Smirnov *et al*., 2002).

Substantially smaller networks in the United States have employed a different instrument that monitors aerosols known as the Multifilter Rotating Shadowband Radiometer (MFRSR; Harrison *et al*., 1994). These smaller networks are operated by state and federal agencies and universities. In our analyses, we used data from both the AERONET and MFRSR networks.

3. DATA AND METHODS

3.1. Aerosol data

The AERONET collaboration provides globally distributed observations of aerosol optical properties in geographically diverse aerosol regimes. The data are transmitted from the sites via the GOES and METEOSAT satellite platforms to ground-receiving stations in the United States, Germany, and Japan. Data from AERONET are available online in near real time via a data-processing, display, and analysis system. This system includes an automatic cloud-screening algorithm (Holben *et al*., 1998, 2001).

The Cimel instruments provide τ_a at eight spectral bands between 340 and 1020 nm. We used τ_a derived at 500 nm and α calculated at wavelengths between 440 and 870 nm since these represent the most optically stable wavelengths, particularly at low optical depths (Smirnov *et al*., 1996; Holben *et al*., 2001). The AERONET τ_a and α data were available as instantaneous observations or as daily averages. We used daily averaged data since our goal was to produce aerosol climatologies. Daily averages were also compatible with the meteorological data used in subsequent analyses.

A total of 20 stations across North America having at least 3 years of reliable AERONET data records were used in this research (Figure 1, Table I). The earliest records commenced in 1993. Across all stations, the periods of record ranged between 3 and 10 years, with an average duration of 6.1 years. These 20 sites represent a diverse array of environments including rural, urban, suburban, and forested locations within

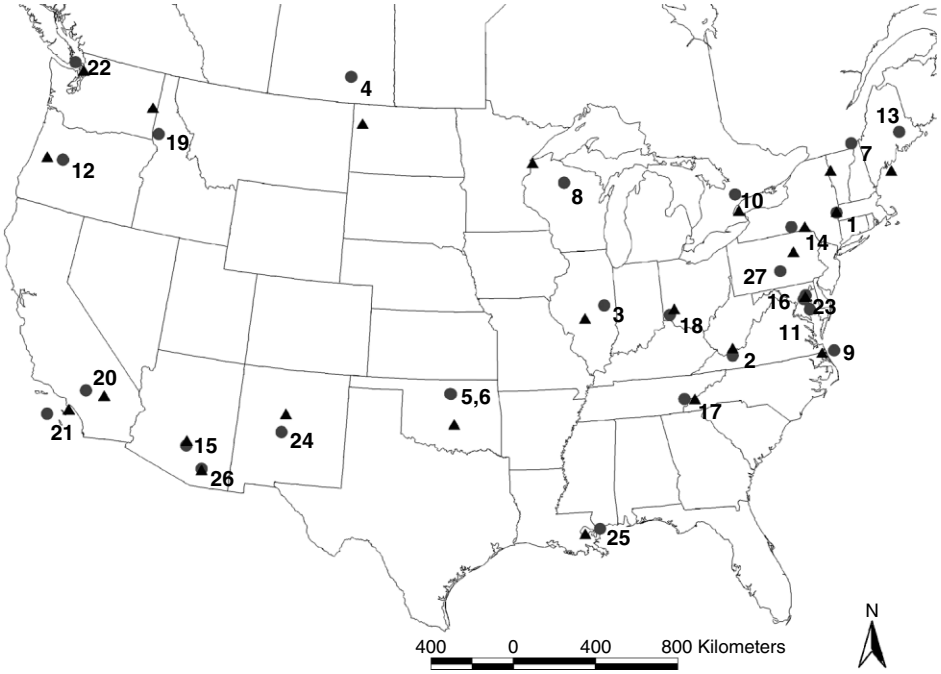

Figure 1. Locations of aerosol-monitoring sites (circles) and SSC stations (triangles) used in this study. Site numbers correspond to Table I

desert, marine west coast, Mediterranean, humid continental, humid subtropical, steppe, and subarctic climatic environments.

Optical data were also available from nine MFRSR stations where the period of record was at least 3 years (Figure 1, Table I). The records ranged between 5 and 12 years, the average duration was 7.3 years, and the earliest observations commenced in 1992. However, unlike AERONET the MFRSR, data for these stations were in the form of total optical depth (τ), rather than aerosol optical depth (τ_a). Total optical depth is the sum of the optical depths of molecules (Rayleigh scattering), gases, and aerosols, i.e. τ represents the total attenuation of the atmosphere. The MFRSR instruments measure irradiance at six nominal wavelengths, including 500 nm. At five of these wavelengths, the influence of water vapor and oxygen absorption is negligible. Thus, we calculated τ_a at each of these wavelengths by subtracting from τ the optical depths due to Rayleigh scattering (τ_r) and ozone absorption (τ_o). The Rayleigh optical depth was calculated according to Hansen and Travis (1974) as a function of wavelength and daily averaged surface pressure. The ozone optical depth was determined from daily averaged total column ozone (u_o) and the ozone absorption coefficients (A_o) tabulated in Shettle and Anderson (1995). Daily average u_o for each site was determined from the algorithm of Van Heuklon (1979). Having calculated τ_a, we determined α from Ångström's classic equation (Ångström, 1929, 1930).

We were therefore able to acquire or calculate time series of daily averaged τ_a and α for 29 stations across North America. At three locations, MFRSRs and AERONET Cimels were operated in close proximity. At Howland, Maine, and Bondville, Illinois, the MFRSR and AERONET records did not overlap; we merged the two data sets to form one record for each station. At the Cloud and Radiation Testbed (CART) site in Oklahoma, the two periods of record overlapped with good agreement between the data sets; these two sites were retained as two separate records. Thus, we effectively had data for 27 stations (Figure 1). From these data, we constructed preliminary aerosol climatologies for each station by calculating monthly and annual summary statistics of both τ_a (at 500 nm, hereafter referred to as τ_{a5}) and α. We also classified each site as being urban or nonurban.

Table I. Information on the 27 monitoring sites used in this study. For 'Network', A = AERONET, M = MFRSR, and AM refers to a merger of records from both networks. 'Distance' is between the SSC and aerosol-monitoring stations (km), and elevation pertains to the aerosol-monitoring site (m ASL). Site number corresponds to Figure 1

Number	Monitoring site	Nearest locality	Network	SSC station	Distance	Elevation	Period of record	
							Start	End
1	Albany	Albany, NY	M	Albany, NY	8	85	1992	2002
2	Bluefield	Bluefield, WV	M	Beckley, WV	60	823	1992	2001
3	Bondville	Bondville, IL	AM	Springfield, IL	114	212	1992	2002
4	Bratts Lake	Wilcox, SK	A	Williston, ND	244	586	1999	2002
5	CART (Aeronet)	Lamont, OK	A	Oklahoma City, OK	176	315	1996	2002
6	CART (MFR)	Lamont, OK	M	Oklahoma City, OK	176	315	1992	2003
7	CARTEL	Sherbrooke, PQ	A	Montreal, PQ	155	300	1995	2003
8	Chequamegon	Park Falls, WI	A	Duluth, MN	179	515	1999	2001
9	COVE	Hampton, VA	A	Norfolk, VA	44	37	1999	2003
10	Egbert	Egbert, ON	A	Toronto, ON	62	264	1999	2003
11	GSFC	Greenbelt, MD	A	Baltimore, MD	25	50	1995	2002
12	HJ Andrews	Blue River, OR	A	Eugene, OR	80	830	1995	2003
13	Howland	Orono, ME	AM	Brunswick, ME	166	100	1992	2003
14	Ithaca	Ithaca, NY	M	Binghamton, NY	57	503	1992	1995
15	Maricopa	Maricopa, AZ	A	Phoenix, AZ	41	360	2000	2003
16	MD Science Center	Baltimore, MD	A	Baltimore, MD	8	15	1999	2003
17	Oak Ridge	Oak Ridge, TN	M	Knoxville, TN	28	380	1992	1997
18	Oxford	Oxford, OH	M	Dayton, OH	61	285	1992	1995
19	Rimrock	Genesse, ID	A	Spokane, WA	134	824	2000	2003
20	Rogers Dry Lake	Edwards, CA	A	Daggett, CA	85	680	2000	2003
21	San Nicholas	San Nicholas Is., CA	A	Los Angeles, CA	131	133	1998	2003
22	Saturna Island	Saturna Island, BC	A	Whidby Is., WA	58	200	1999	2002
23	SERC	Edgewater, MD	A	Baltimore, MD	70	10	1994	2002
24	Sevilleta	Sevilleta, NM	A	Albuquerque, NM	80	1477	1994	2003
25	Stennis	Stennis, MS	A	New Orleans, LA	70	20	2000	2002
26	Tucson	Tucson, AZ	A	Tucson, AZ	9	779	1993	2001
27	University Park	University Park, PA	M	Williamsport, PA	103	375	1992	2001

3.2. Meteorological data

All previously published studies that have evaluated the influence of meteorological conditions upon aerosol variability have either utilized individual weather parameters or incorporated synoptic classification schemes that relied upon a subjective, manual interpretation of individual weather maps. Here, we used a new weather-type classification scheme that is automated and spatially cohesive. This system, known as the *Spatial Synoptic Classification* (SSC; Sheridan, 2002), is a hybrid classification scheme (Frakes and Yarnal, 1997) that includes an initial, manual identification of weather types, followed by an automated classification based upon these identifications.

Using surface weather data only (namely, air temperature, dew point temperature, sea-level pressure, wind speed and direction, and cloud cover), the scheme classifies each day at a location into one of six weather types (described below). While most weather types inherently suggest a source region, they are limited to surface conditions at a location and thus capture a true measure of ambient meteorological conditions at a particular site. Thus, these are more aptly labeled 'weather types' rather than 'air masses'. The appeal of this classification scheme, besides its automation, is the enhanced spatial cohesiveness among weather stations compared to previous classification schemes (Sheridan, 2002). The SSC has been used in other environmental analyses that assessed the effects of weather type on snow cover anomalies (Leathers *et al*., 2002), snow-water equivalent anomalies (Grundstein, 2003), variability in human mortality (Sheridan and Dolney, 2003), and the magnitude of the urban heat island (Sheridan *et al*., 2000). A similar but earlier classification scheme, the temporal synoptic index (TSI), was used to assess pollutant levels in Philadelphia (Kalkstein and Corrigan, 1986) as well as pollutant transport from the Navajo Generating Station in Arizona (Kalkstein and Webber, 1991). The six weather types are as follows.

- Dry Polar (DP) air is largely synonymous with the traditional continental polar (cP) air mass classification. It is characterized by cool or cold dry air and, for much of the continent, northerly winds. Skies typically feature little or no cloud cover. This weather type has its source in northern Canada and Alaska, and it is advected into the rest of North America by a cold-core anticyclone that emerges from the source region.
- Dry Moderate (DM) air is mild and dry. This weather type has no traditional source region. In the eastern and central portions of North America, DM usually appears with zonal flow aloft, which permits air to traverse the Rocky Mountains and dry and warm adiabatically. It is analogous to the Pacific air mass identified by Schwartz (1991) and others. In other cases, however, it may reflect a significantly modified DP weather type or the influence of more than one weather type.
- Dry Tropical (DT) air is associated with the hottest and driest conditions, and clear skies. It is analogous to the traditional continental tropical (cT) designation. Most commonly, it is present at, or advected from, its source region, which includes the deserts of the southwestern United States and northwestern Mexico. It can also be produced by strong downsloping winds, where rapid compressional heating can produce desert-like conditions.
- Moist Polar (MP) air is a large subset of the traditional maritime polar (mP) air mass. Weather conditions are cool, cloudy, and humid, often with light precipitation. This can appear via inland advection of air from the North Pacific or North Atlantic. It can also arise where there is frontal overrunning well to the south, or when a cP air mass acquires moisture while traversing a cool water body.
- Moist Moderate (MM) air is warmer and more humid than MP air, though also cloudy. This can form either as a modified mP air mass or as independently south of MP air nearer a warm front. During summer, it can also occur under the influence of maritime tropical air masses on days with high cloud cover.
- Moist Tropical (MT) air is analogous to the traditional maritime tropical (mT) air mass. It arrives in North America via the Gulf of Mexico or the tropical Pacific or Atlantic Oceans. This weather type is warm and very humid, cloudy in winter, and partly cloudy in summer. Convective precipitation is quite common, especially in summer.

These six weather types comprise the SSC catalog, along with a transitional (TR) situation, which represents a day in which one weather type yields to another, based on large diurnal changes in dew point temperature, pressure, and wind. Mean conditions associated with each of these SSC weather types, as well as other information, can be found on the SSC homepage (http://sheridan.geog.kent.edu/ssc.html).

Daily SSC calendars have been developed for over 300 stations across North America, for periods ranging up to 60 years, and are updated continuously. In this analysis, each AERONET and MFRSR site is evaluated with weather types from the nearest SSC station whose period of record includes that of the aerosol-monitoring site. The mean distance between each aerosol and SSC station pair is 90 km, with a maximum distance of 244 km (Table I).

3.3. Methods of analysis

Once the SSC and aerosol data sets were merged, analysis began with a calculation of mean values of both τ_{a5} and α. For each of the two variables, statistics were calculated for the year as a whole at each site. The data sets were then subdivided and analyzed on a monthly level, as well as on a seasonal level, defined meteorologically, e.g. winter as December, January, and February.

Mean values of τ_{a5} and α were also calculated for each of the SSC weather types at the annual and seasonal levels. To assess the appropriateness of stratifying days via the SSC, we utilized the nonparametric Kruskal–Wallis H test to compare the similarity of the distributions of both τ_{a5} and α across the seven weather types. Owing to the large variability in distribution across weather types, a parametric test such as Analysis of Variance (ANOVA) was not appropriate (Rogerson, 2001). Each of the four seasons was evaluated separately; monthly evaluations were not performed because of sample-size considerations, particularly during the winter months.

Our initial work yielded 27 different aerosol climatologies, i.e. one at each site. To evaluate the spatial cohesiveness of these results, we performed several cluster analyses. Cluster analysis has been used with aerosol data to group days with similar observations at one site (Treffeisen *et al*., 2004). In this research, however, we utilize cluster analysis to group stations with like climatologies into regions. To our knowledge, this methodology has not previously been applied to aerosol data. However, cluster analysis applied at the station level has been utilized in myriad other climatological applications, including defining agricultural regions (e.g. Holden and Brereton, 2004) or mesoscale climate regions (e.g. De Gaetano, 1996).

For the cluster analyses we analyzed τ_{a5} and α separately. For clusters based on SSC frequencies, at each site we gathered 28 variables (seven weather types for each of four seasons) that represent the mean values of τ_{a5} (or α) for the particular season-weather type (e.g. winter DM mean τ_{a5}, winter DP mean τ_{a5} etc.). To mitigate multicollinearity among these variables, the 28 were reduced utilizing unrotated principal components analysis. Unrotated components are appropriate when the goal is to cluster the resultant components rather than interpret them (Yarnal, 1993). All components with eigenvalues over 1 were retained, resulting in seven transformed variables retained for both τ_{a5} and α. We experimented with several different means of clustering, all of which yielded similar results. The results of k-means cluster analysis (Yarnal, 1993), a nonhierarchical, iterative procedure, are presented here. In k-means analysis, all stations are originally assigned to one of k categories, and a centroid is then calculated for each category. The process then iterates, and any single station can migrate to a different category should it be closer to another category's centroid. Using one-way ANOVA on the monthly means across all clusters, we confirmed that in all cases there were statistically significant differences among at least one of the clusters. Subsequent t-tests compared all identified clusters of $n > 2$ and confirmed that there were statistically significant differences among all groups in all of the transformed variables ($p < 0.01$). Five clusters were retained for both τ_{a5} and α; for τ_{a5} there are three clusters of size $n > 2$, for α there are two.

Similarly, we produced cluster maps on the basis of seasonal means of τ_{a5} and α irrespective of the τ_{a5} SSC class. For both of these cases, the four variables (one for each season) were reduced to two via principal components analysis before being clustered.

4. RESULTS AND DISCUSSION

4.1. Spatial and seasonal variability in α and τ_{a5}

Although we were able to evaluate aerosol data from 27 stations, Figure 1 illustrates the nonuniform distribution of stations across the North American continent. For instance, there are no aerosol-monitoring stations (where the period of record exceeded 3 years) in the High Plains states and many of the Midwestern states, while there is clearly a cluster of stations in the eastern part of the continent. This spatial constraint notwithstanding, in general, turbidity is lowest in the west and southwest and highest in the east, especially over the mid-Atlantic states (Figure 2). Annually averaged τ_{a5} ranges from 0.08, observed at HJ Andrews (Site 12 on Figure 1), San Nicholas Island (Site 21), Saturna Island (Site 22), Sevilleta (Site 24), and Tucson

(Site 26) to 0.32 at the Maryland Science Center (Site 16; Table II). This spatial distribution of aerosols likely reflects the influence of higher emissions of anthropogenic aerosols in the eastern region of the United States (United States Environmental Protection Agency (US EPA), 2004) although the frequency of weather types may also influence this spatial pattern (discussed in Section 4.2).

Annually averaged α ranges from 0.69 at Ithaca (Site 14) to 1.82 at Egbert (Site 10; Table II). The smallest aerosols (largest α) were observed in urban mid-Atlantic and northeast areas (Figure 3). This is likely due to the higher rate of emission of anthropogenic aerosols in those regions (US EPA, 2004), which are relatively small in size. In general, the largest aerosols (smallest α) appear in two regions: the industrial Midwest and the west/southwest. In the former region, these aerosols may be of agricultural origin, for example, aerosols generated from windblown soils in the upper Midwest transported downwind. Across the southwest, large aerosols are likely of desert origin. The small aerosols observed at the Egbert site, which is classified as nonurban, may be due to its proximity to Toronto (62 km).

Interestingly, the two sites in California (Rogers Dry Lake and San Nicholas Island, Sites 20 and 21) do not appear to be strongly influenced by anthropogenic emissions (pollution) from the Los Angeles basin – despite its proximity – since the aerosol size is relatively large and τ_{a5} is relatively small. Instead, the aerosol environment at San Nicholas Island, located 145 km southwest of Los Angeles, is likely heavily influenced by marine aerosols generated by the prevailing westerlies. Rogers Dry Lake is located 160 km northeast of Los Angeles in the Mojave Desert. It is most likely capturing relatively large desert or rural aerosols from the San Joaquin Valley. This monitoring site is also located to the north of the San Gabriel mountains, which provide a natural barrier to airflow from the Los Angeles basin. The patterns at San Nicholas Island and Rogers Dry Lake are consistent with reports of local *versus* regional contributions to mass concentrations of aerosols. The US EPA (2004) reports that the majority of inhalable aerosol mass in the western United States is of local origin.

In contrast, the COVE (CERES Ocean Validation Experiment) site in Virginia (Site 9), located on an ocean platform 25 km offshore, does appear to be influenced by the metropolitan areas along the mid-Atlantic seaboard. Its relatively high long-term τ_{a5} (0.22) and α (1.62) suggest it is influenced more by aerosols of anthropogenic origin than marine origin despite its maritime location. These optical values are similar to those

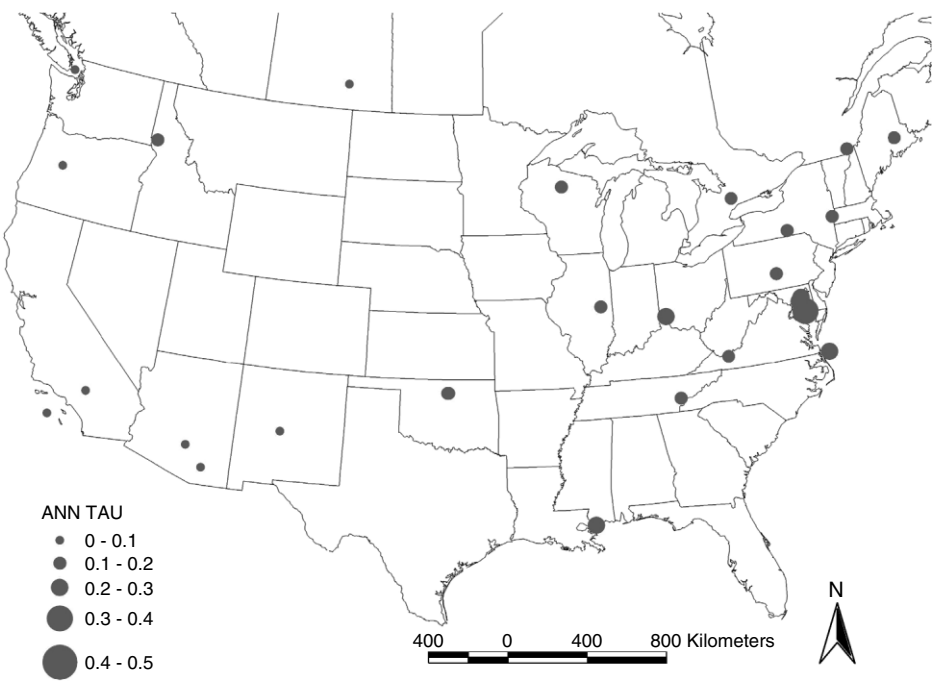

Figure 2. Mean annual values of τ_{a5}

Table II. Mean annual values of τ_a and α, and site characteristics, for the 27 sites evaluated. Site number corresponds to Figure 1

	Monitoring site	τ_{a5}	α	Site characteristic
1	Albany	0.16	1.41	Urban
2	Bluefield	0.17	1.10	Urban
3	Bondville	0.20	0.96	Nonurban
4	Bratts Lake	0.09	1.37	Nonurban
5	CART	0.12	1.11	Nonurban
6	CART	0.17	1.38	Nonurban
7	CARTEL	0.15	1.50	Urban
8	Chequamegon	0.13	1.22	Nonurban
9	COVE	0.22	1.62	Nonurban
10	Egbert	0.15	1.82	Nonurban
11	GSFC	0.24	1.70	Urban
12	HJ Andrews	0.08	1.58	Nonurban
13	Howland	0.13	1.68	Nonurban
14	Ithaca	0.18	0.69	Nonurban
15	Maricopa	0.10	1.16	Nonurban
16	MD Science Center	0.24	1.79	Urban
17	Oak Ridge	0.19	1.04	Urban
18	Oxford	0.21	1.01	Nonurban
19	Rimrock	0.11	1.33	Nonurban
20	Rogers Dry Lake	0.09	1.13	Nonurban
21	San Nicholas	0.08	1.21	Nonurban
22	Saturna Island	0.08	1.48	Nonurban
23	SERC	0.32	1.72	Nonurban
24	Sevilleta	0.08	1.37	Nonurban
25	Stennis	0.22	1.54	Nonurban
26	Tucson	0.08	1.04	Urban
27	University Park	0.19	1.11	Nonurban

observed at other stations in nearby Maryland including GSFC (Goddard Space Flight Center), in Greenbelt, Site 11), Maryland Science Center (Baltimore, Site 16), and SERC (Smithsonian Environmental Research Center, in Edgewater, Site 23). Unlike western locations, in the east, regional pollution contributes more than half of the mass of inhalable aerosols (US EPA, 2004).

Both aerosol parameters display seasonal patterns as well. Of the two, τ_{a5} is associated with a much more distinct seasonal variability (Figure 4, $p < 0.001$). On comparing the monthly mean values of τ_{a5} across all 27 stations, a relatively linear increase from a median of 0.08 in December and January to a median of 0.21 in June is observed. Summer values remain high before a step downward in September. This seasonal cycle of a summer maximum and a winter minimum has been well documented in previous research (e.g. Power and Willmott, 2001; Power, 2003; Power and Goyal, 2003) and likely reflects greater specific humidity and atmospheric convection during the warmer time of year, increasing turbidity as a result (discussed in Section 4.2). Along with this overall increase is a large increase in station-to-station variability during the warm season as well. Interestingly, this increase appears less linear, featuring the largest range of station means during June, July, and August; moderately large variability in May and September; and relatively similar levels of variability across all other months. The very high station averages during the three summer months are observed at the three Maryland sites discussed above (Sites 11, 16, and 23).

In contrast, the seasonal pattern and variability in α are much less distinct (Figure 5), although there is still a statistically significant difference across months ($p = 0.001$). On a monthly level, there are lower values of α during the first half of the year, with significantly lower values during the months of April and May, suggesting a general increase in larger-sized aerosols during this period. Variability from station-to-station

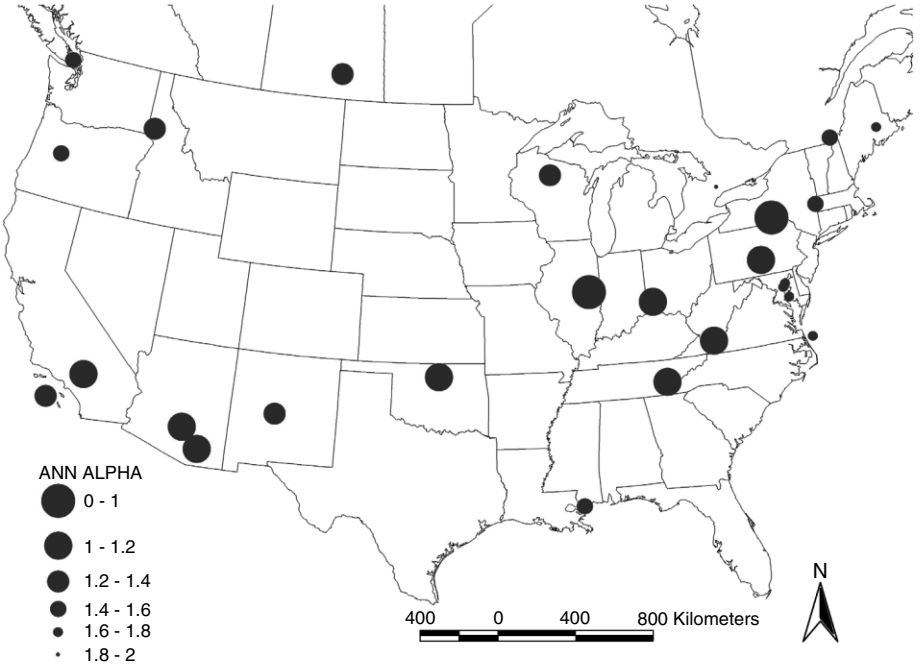

Figure 3. Same as Figure 2, except for α

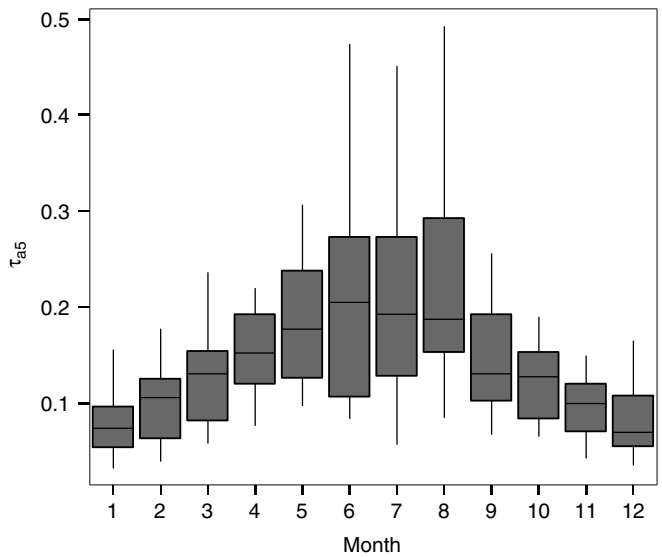

Figure 4. Boxplot depicting median and variability of the mean monthly values of τ_{a5} across all stations

does not follow the seasonal pattern as it does with τ_{a5}; rather, generally higher variability is observed during the cold half of the year.

4.2. Synoptic variability

To further elucidate the spatial and temporal patterns discussed above, we evaluated the differences in τ_{a5} and α across SSC categories for each station on an annually averaged basis, as well as stratified by season. The distributions of both τ_{a5} and α were compared across all weather types.

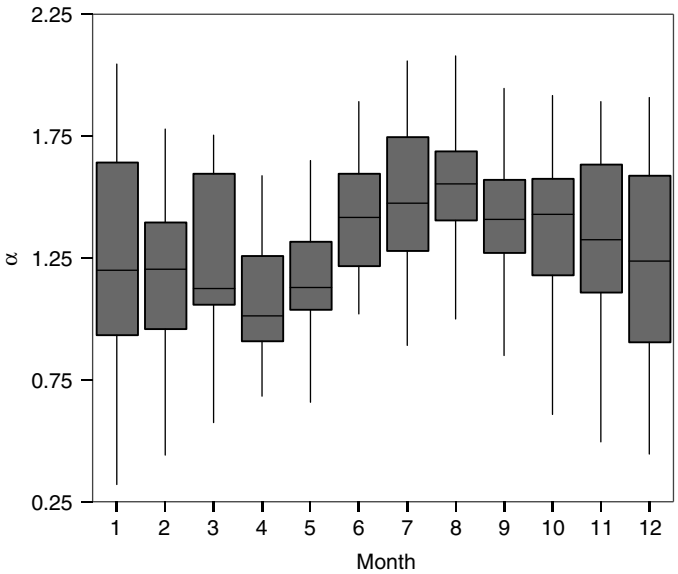

Figure 5. Same as Figure 4, except for α

4.2.1. τ_{a5}. Averaged annually and across all stations, τ_{a5} generally increases with the temperature and humidity of the weather type. For instance, the aerosol optical depth is lowest during DP weather types (mean τ_{a5}, 0.10) and highest during MT weather types (mean τ_{a5}, 0.26). The higher humidity associated with MT conditions enhances hygroscopic growth of aerosols (Pilinis *et al*., 1995; Kotchenruther *et al*., 1999; Kay and Box, 2000; Smirnov *et al*., 2000; Malm and Day, 2001), while strong surface heating associated with MT weather types initiates convection. This, in turn, serves to increase the particle flux from the ground via entrainment (Al-Jamal *et al*., 1987; Pedrós *et al*., 1999). Higher insolation may also enhance photochemical conversion of gases to aerosols (Peterson and Flowers, 1977; Holben *et al*., 2001). All three of these processes will be maximized under MT weather types and will thus enhance τ_{a5}. With the DP weather type, in contrast, these processes are absent or weak, with much lower specific humidity and much greater atmospheric stability. Further, DP weather types originate from northern Canada and Alaska where the anthropogenic aerosol load is likely to be quite low.

When stratified by season, τ_{a5} shows significant differences across SSC types (Table III). This synoptic variability is most readily observed during the summer and autumn months when more than three-fourths of all sites show statistically significant differences in distributions across the SSC types. During winter and spring, these percentages are somewhat lower. Sites not associated with statistically significant differences in general have either a very low τ_{a5} sample size for a particular season (a significant problem across much of the north, especially northwest, during winter) or a predominance of one weather type (e.g. MT across the Gulf Coast during the summer), which limits the sample size of other weather types.

The synoptic variability in aerosol properties is superimposed on the seasonal pattern described above (Figure 6). Thus, τ_{a5} in winter during DP weather types are low (mean τ_{a5} is 0.08; Figure 7) compared to τ_{a5} in summer during DP (0.14). This is likely because the thermal and moisture conditions of DP are exaggerated in winter compared to summer, i.e. the DP atmosphere in winter is even drier and colder than it is in summer, and it is usually associated with a strong inversion. Thus, the likelihood of hygroscopic growth of aerosols, convection, and entrainment of aerosols and photochemical growth of aerosols is minimal. At the other extreme, τ_{a5} during MT in summer is relatively high (Figure 8); the mean summer τ_{a5} is 0.30 averaged across all stations, with a maximum of 0.60 at Maryland Science Center (Site 16) and SERC (Site 23). The warmer and more humid conditions of an MT in summer are highly conducive to the growth, entrainment, and formation of aerosols. The next highest seasonally averaged τ_{a5} occurs with the DT weather type in summer (mean τ_{a5} is 0.25; Figure 6). While the role of hygroscopic growth of aerosols in a summer DT is

Table III. The percentage of stations that show statistically significantly different distributions across SSC categories, stratified by season

Season	τ_{a5} (%)	α (%)
Winter	67	37
Spring	56	30
Summer	78	78
Autumn	78	70

likely to be relatively low, the hot, dry conditions and clear skies associated with this weather type suggest that entrainment by convection likely plays a key role in the higher turbidity.

When analyzing the output of our cluster analyses, regional and synoptic variability in τ_{a5} emerged. Five clusters are identified (Figure 9). Clusters 1 through 3 include 25 of the 27 sites; mean profiles are depicted in Figure 10. Cluster 1 includes 12 stations, including all stations west of the High Plains. This 'Western' cluster is associated with relatively low values year-round, as discussed above, and, in general, lesser variability across weather types. With one exception (Tucson, Site 26), all of the stations in Cluster 1 are nonurban. As articulated earlier, the majority of inhalable aerosol mass in the western United States is of local rather than regional origin. Furthermore, aerosol emission sources are more concentrated in the east than in the west (US EPA, 2004). The relatively low turbidity associated with this western cluster likely reflects the remoteness of these stations to significant aerosol sources and the fact that the aerosols are not transported as far as those in the east, regardless of weather type.

Collectively, Clusters 2 and 3 include most of the eastern stations. The 'Industrial' Cluster 2 encompasses most sites within the Midwestern and Mid-Atlantic regions, where there is a higher density of aerosol emission sources. Within this cluster, substantially higher τ_{a5} values are observed across all weather types compared to the western cluster. The distinction among the weather types is also greater, with noticeably higher values across those types associated with significant convection (MM, MT, and DT). On comparing Clusters 1 and 2, there is a stronger synoptic influence on τ_{a5} when τ_{a5} is relatively high. Excluding island stations (San Nicholas and Saturna Islands), the mean elevation of Cluster 1 stations is 647 m, while the mean elevation of Cluster 2 stations is 335 m. A regression analysis (inclusive of all stations analyzed) between τ_{a5} and elevation shows a statistically significant relationship ($p = 0.001$) between these two variables, suggesting that station elevation may play a role in turbidity. These patterns are consistent with relationships described by Ingold

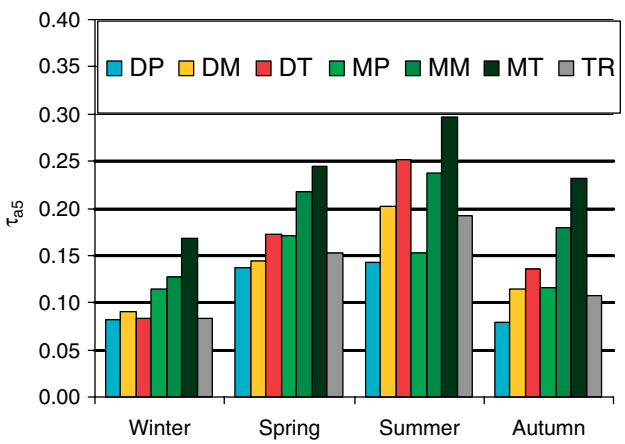

Figure 6. Seasonal variability in mean τ_{a5} by SSC

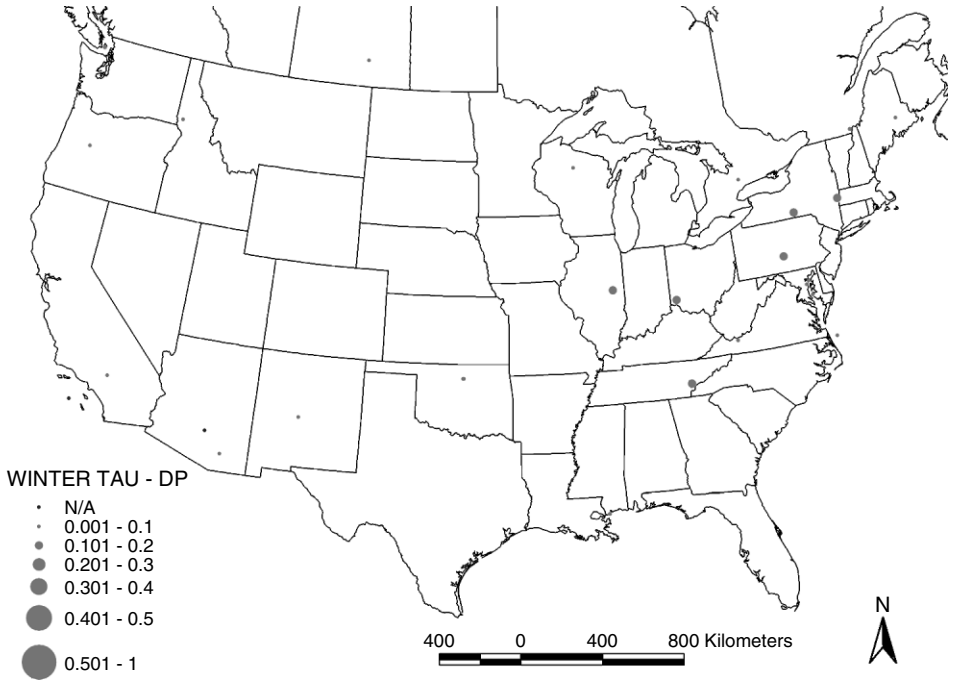

Figure 7. Mean τ_{a5}, winter, dry polar (DP) weather type

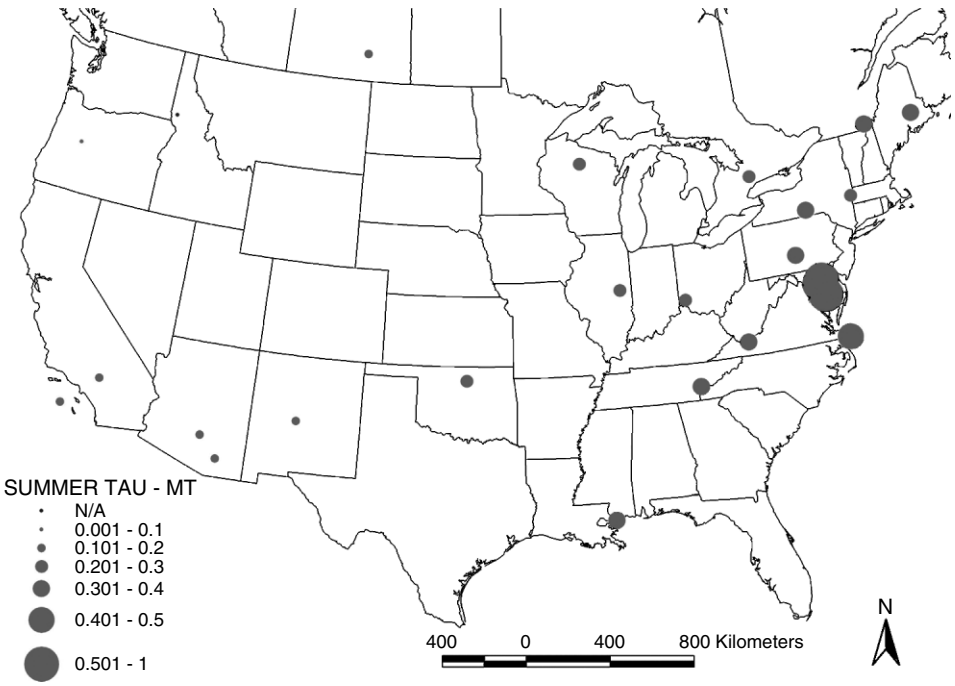

Figure 8. Mean τ_{a5}, summer, moist tropical (MT) weather type

et al. (2001). These investigators reported weaker links between τ_{a5} and synoptic airflows in Switzerland when τ_{a5} was low than when τ_{a5} was high. They also reported a lower τ_{a5} at higher elevations, which they attributed to the fact that the origin of the aerosols is the planetary boundary layer.

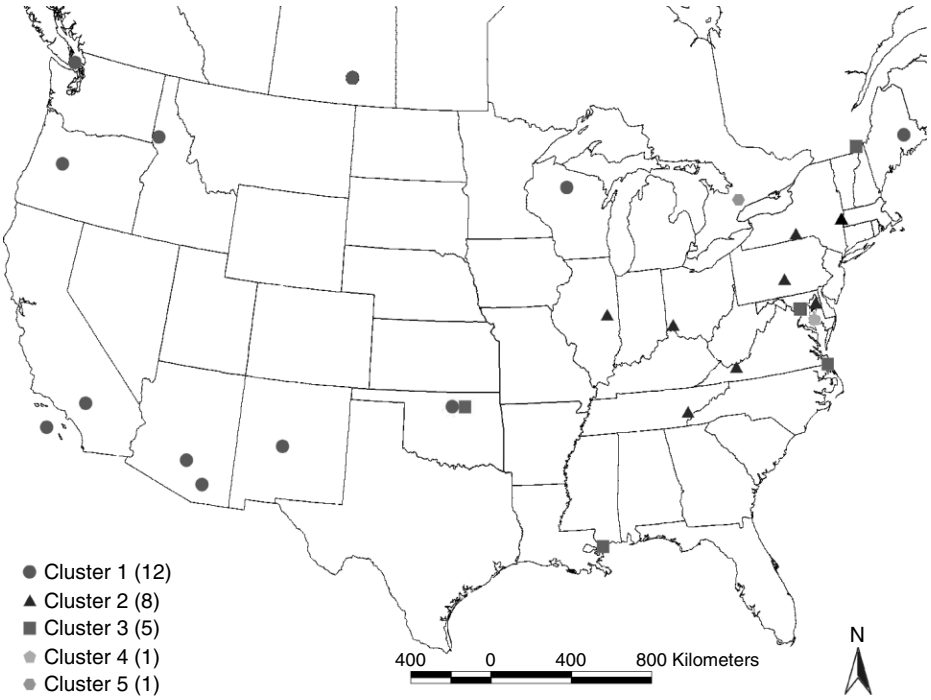

Figure 9. Clusters of sites with similar SSC- and season-stratified τ_{a5} means

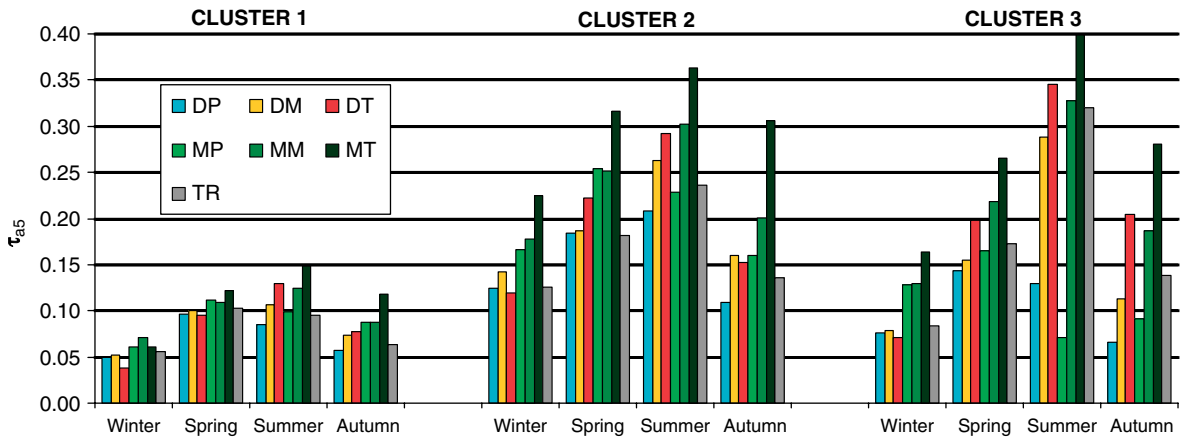

Figure 10. Mean seasonally and synoptically stratified τ_{a5} values for Clusters 1, 2, and 3 from Figure 9

The 'Eastern Peripheral' Cluster 3 includes five stations that surround the Industrial cluster. These five stations are associated with lower τ_{a5} values than the Industrial cluster but with the largest synoptic variability of any cluster. The polar weather types DP and MP have significantly lower τ_{a5} values that are closer in magnitude to those in the Western cluster. This may reflect the relatively clean pathways followed by the air masses associated with DP and MP weather conditions, i.e. from the continental north or the North Atlantic. With other weather types, most notably MM and MT, but also DT and DM during the warmer times of year, mean τ_{a5} values approach those of the Industrial cluster. Both the Industrial and Eastern Peripheral clusters consist of a mixture of urban and nonurban stations, indicating the regional nature of turbidity in the eastern part of the continent. In the case of Site 6 (CART), which is nearly collocated with the Cluster 1 Site 5, the different period of record (Table I) may explain the appearance of Site 6 in this cluster.

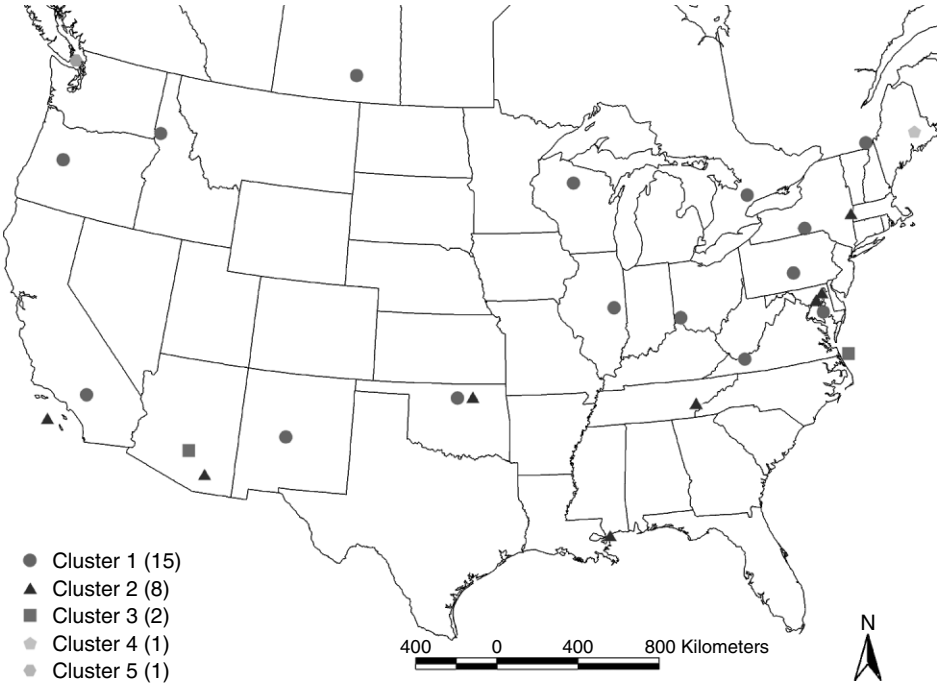

Figure 11. Clusters of sites with similar SSC- and season-stratified α means

Clusters 4 and 5 each contain one site: SERC (Site 23) and Egbert (Site 10) respectively. Both these sites are associated with a synoptic pattern similar to Cluster 2, although one or more weather types contain a highly anomalous τ_{a5} value that forces it into another cluster. As these patterns do not occur at more than one station, and within-station synoptic variability is inconsistent, we believe them to be individual outliers and are uncertain as to the cause of the discrepancy.

4.2.2. α. In comparison with τ_{a5} the variability in α across weather types is smaller when averaged annually and across all stations. Relatively larger aerosols are associated with the two polar weather types – Maritime Polar (MP) and DP – where the mean α for both types is 1.31. The smallest aerosols are associated with the MT weather type, with a mean α of 1.48. Since the variability in annually averaged α is small and the mean α is calculated across many locations with different physical characteristics, it is difficult to attribute this synoptic variability to any particular physical process. However, in analyzing the synoptic variability by season, differences are much less significant across the different weather types; rather, the α values reflect the overall seasonal pattern in Figure 5, with higher values in summer and autumn, and lower values especially in spring, but also in winter. Fewer stations are associated with statistically significant changes across SSC categories, most notably in winter and spring (Table III). Thus, it appears that these overall differences in α merely reflect the seasonality of weather types. As DP is much more common in winter and MT is more common in summer (Sheridan, 2002), and the mean α is larger in summer than in winter, the mean α of MT is larger than DP.

In analyzing our cluster analyses of α values, once again the results are less clear than they are with τ_{a5}. Five clusters are again identified (Figure 11), though only Clusters 1 and 2 contain more than two stations. The cluster means (Figure 12) display a lack of consistency across weather type and merely identify greater seasonal variability in Cluster 1 (sites associated with larger aerosols, and hence lower α values, in winter and spring) and less seasonal variability in Cluster 2. Geographically, most of the Cluster 2 stations appear to the south of Cluster 1 stations. However, we are not aware of any physical explanation as to why aerosols, on average, are smaller at the southern (Cluster 2) stations than at Cluster 1 stations. In short, the physical bases behind the synoptic and spatial variability in α are less evident than for τ_{a5}.

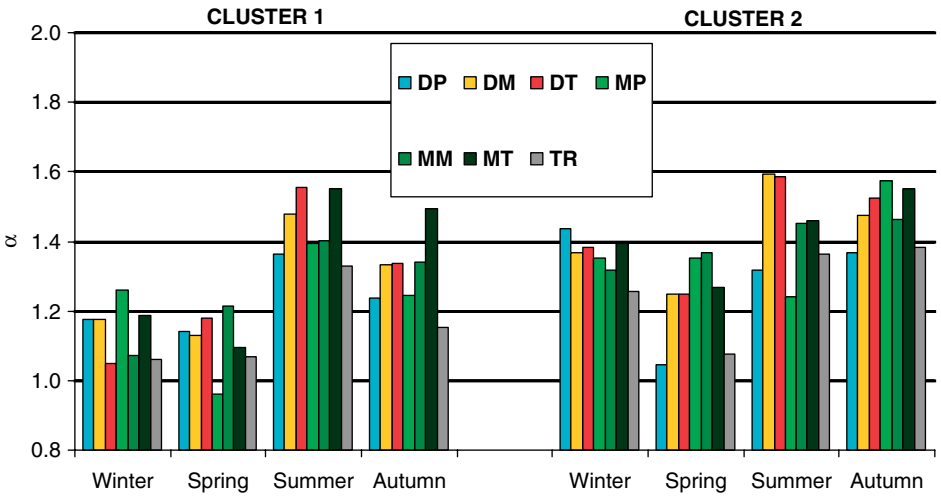

Figure 12. Mean seasonally and synoptically stratified α values for Clusters 1 and 2 from Figure 11

4.3. Aerosol sampling biases

Earlier, we discussed the constraints associated with aerosol-monitoring techniques that result in gaps in the turbidity record, and we asserted that aerosol climatologies derived from clear-sky data may not be representative. Table IV illustrates this bias for the CARTEL aerosol site (Site 7) in Sherbrooke, Quebec. Here, we compare the SSC frequency (recorded at the Montreal SSC station) for the entire period of record (1995–2002) with the SSC frequency on days for which aerosol measurements are available. It is quite clear that aerosol sample days at CARTEL are not representative of the overall synoptic variability of the location. The clearer weather types, most notably DM and DT, are overrepresented in the data set, the latter by more than a factor of 2. Conversely, the weather types that are associated with more humid and cloudier conditions are underrepresented in the data set. Most notable is the MP weather type, which within the aerosol climatology only occurs one-fifth as often as it does throughout the full period of record. Interestingly, the MT weather type is overrepresented within the aerosol data set at CARTEL, despite its high humidity. During much of the year MT is cloudy; however, during midsummer, when the weather type is most common here, it is highly convective, suggesting that over the course of a day (most likely during the morning hours) there is some opportunity for an aerosol measurement to be taken, before the convective cloud cover builds.

Table IV. Comparative frequencies of SSC weather type. 'Frequency, all days' refers to the frequency of SSC weather type across all days at Montreal for the 8-year period. 'Frequency, aerosol obs.' refers to the frequency of SSC weather type at Montreal across only those days for which aerosol observations are available at CARTEL (Site 7, Figure 1). Ratio is the ratio of aerosol observation days to all days

SSC weather type	Frequency all days 1995–2002	Frequency aerosol obs. 1995–2002	Ratio
Dry Moderate	25.2	38.0	1.51
Dry Polar	20.9	25.0	1.19
Dry Tropical	1.9	4.7	2.44
Moist Moderate	18.8	7.4	0.39
Moist Polar	14.8	2.8	0.19
Moist Tropical	8.1	11.9	1.47
Transitional	10.3	10.3	1.00

Similar biases exist at other stations, with more pronounced biases in locations where mean cloud cover is greater. We argue that aerosol climatologies derived from such data are therefore unrepresentative.

5. CONCLUSIONS AND FUTURE DIRECTIONS

In this research, we have analyzed the spatial variability of two aerosol variables, the spectral aerosol optical depth at 500 nm (τ_{a5}), and Ångström's wavelength exponent (α) across 27 North American stations. The number of stations, as well as the mean period of record at each station, far exceeds those analyzed in any single previously published study. The results from our overall analyses yield conclusions similar to that of much previous research: turbidity is much greater over the eastern portions of the continent, and lesser out west and farther north, away from more heavily industrialized regions. Seasonality of both parameters, especially τ_{a5}, was shown, with a greater optical depth of aerosols during the summertime, coinciding with higher levels of specific humidity and atmospheric turbulence.

Our research further analyzed aerosol variability according to synoptic situation. Via the SSC, we have uncovered significant differences across these weather types, once again much more significant with τ_{a5} than with α. The moist weather types, especially Moist Tropical, display considerably higher τ_{a5} values, while the colder, drier Dry Polar weather type is associated with the lowest τ_{a5}. Certain weather types show considerable seasonal variability; the warm to hot Dry Tropical weather type is associated with relatively low values in winter, but high values in summer, when convection is extreme.

In future work we will first develop stratifications according to lower-tropospheric (850 hPa) atmospheric flow and compare them with aerosol properties, as we did with the SSC in this research. We will then combine the synoptic climatology that is presented here with our tropospheric flow analyses and attempt to develop a more representative aerosol climatology for each station. It is important to note in Table IV that the cloudier synoptic situations, though underrepresented, are still represented within the data set. Thus, while acknowledging the greater uncertainty due to smaller sample size, estimations may be made for days in the data set for which aerosol observations are unavailable. Our goal will be to construct near-continuous time series of τ_a, and perhaps α, at each station and, in turn, more reliable aerosol climatologies for North America.

ACKNOWLEDGEMENTS

We thank Brent Holben, Bruce McArthur, Rick Wagener, Alain Royer, Norm O'Neill, John Vande Castle, Jeannette van den Bosch, Robert Frouin, Jay Herman, Maria Tzortziou, Gordon Labow, Doug Moore, Steve Tate, Kurt Thome and their staff of the AERONET program for establishing and maintaining the AERONET sites used in this investigation. We would also like to thank Joseph Michalsky, Alexander Smirnov, and Lynn Shirley for assistance in conducting this research. Financial support from the National Science Foundation (grant BCS0351241) is greatly acknowledged.

REFERENCES

Al-Jamal K, Ayyash S, Rasas M, Al-Aruri S, Shaban N. 1987. Atmospheric turbidity in Kuwait. *Atmospheric Environment* **21**(8): 1855–1859.

Anderson TL, Charlson RJ, Winker DM, Ogren JA, Holmén K. 2003a. Mesoscale variations of tropospheric aerosols. *Journal of the Atmospheric Sciences* **60**(1): 119–136.

Anderson TL, Charlson RJ, Schwartz SE, Knutti R, Boucher O, Rodhe H, Heintzenberg J. 2003b. Climate forcing by aerosols – a hazy picture. *Science* **300**(5622): 1103–1104.

Ångström A. 1929. On the atmospheric transmission of sun radiation and on dust in the air. *Geografiska Annaler* **2**: 156–166.

Ångström A. 1930. On the atmospheric transmission of sun radiation II. *Geografiska Annaler* **2 and 3**: 130–159.

Augustine JA, Cornwall CR, Hodges GB, Long CN, Medina CI, DeLuisi JJ. 2003. An automated method of MFRSR calibration for aerosol optical depth analysis with application to an Asian dust outbreak over the United States. *Journal of Applied Meteorology* **42**(2): 266–278.

Chiapello I, Goloub P, Tanré D, Marchand A, Herman J, Torres O. 2000. Aerosol detection by TOMS and POLDER over oceanic regions. *Journal of Geophysical Research* **105**(D6): 7133–7142.

De Gaetano AT. 1996. Delineation of mesoscale climate zones in the northeastern United States using a novel approach to cluster analysis. *Journal of Climate* **9**(8): 1765–1782.

Deuzé JL, Bréon FM, Devaux C, Goloub P, Herman M, Lafrance B, Maignan F, Marchand A, Nadal F, Perry G, Tanré D. 2001. Remote sensing of aerosols over land surface from POLDER-ADEOS- 1 polarized measurements. *Journal of Geophysical Research* **106**(D5): 4913–4926.

Dubovik O, Smirnov A, Holben BN, King MD, Kaufman YJ, Eck TF, Slutsker I. 2000. Accuracy assessments of aerosol optical properties retrieved from Aerosol Robotic Network (AERONET) Sun and sky radiance measurements. *Journal of Geophysical Research* **105**(D8): 9791–9806.

Eck TF, Holben BN, Ward DE, Dubovik O, Reid JS, Smirnov A, Mukelabai MM, Hsu NC, O'Neill NT, Slutsker I. 2001. Characterization of the optical properties of biomass burning in Zambia during the 1997 ZIBBEE field campaign. *Journal of Geophysical Research* **106**(D4): 3425–3448.

Flowers EC, McCormick RA, Kurfis KR. 1969. Atmospheric turbidity over the United States, 1961–1966. *Journal of Applied Meteorology* **8**(6): 955–962.

Formenti P, Andreae MO, Andreae TW, Galani E, Vasaras A, Zerefos C, Amiridis V, Orlovsky L, Karnieli A, Wendisch M, Wex H, Holben BN, Maenhaut W, Lelieveld J. 2001. Aerosol optical properties and large-scale transport of air masses: observations at a coastal and a semiarid site in the eastern Mediterranean during summer 1998. *Journal of Geophysical Research* **106**(D9): 9807–9826.

Frakes B, Yarnal B. 1997. A procedure for blending manual and correlation-based synoptic classifications. *International Journal of Climatology* **17**(13): 1381–1396.

Ghan SJ, Easter RC, Chapman EG, Abdul-Razzak H, Zhang Y, Leung LR, Laulainen NS, Saylor RD, Zaveri RA. 2001. A physically based estimate of radiative forcing by anthropogenic sulfate aerosol. *Journal of Geophysical Research* **106**(D6): 5279–5293.

Grundstein A. 2003. A synoptic-scale climate analysis of anomalous snow water equivalent over the Northern Great Plains of the USA. *International Journal of Climatology* **23**(8): 871–886.

Halthore RN, Markham BL, Ferrare RA, Aro TO. 1992. Aerosol optical properties over the midcontinental United States. *Journal of Geophysical Research* **97**(D17): 18769–18778.

Hansen J, Travis LD. 1974. Light scattering in planetary atmospheres. *Space Science Reviews* **16**: 527–610.

Harrison L, Michalsky J, Berndt J. 1994. Automated multifilter rotating shadow-band radiometer: an instrument for optical depth and radiation measurements. *Applied Optics* **33**(22): 5118–5125.

Haywood JM, Francis PN, Geogdzhayev I, Mishchenko M, Frey R. 2001. Comparison of Saharan dust aerosol optical depths retrieved using aircraft mounted pyranometers and 2-channel AVHRR algorithms. *Geophysical Research Letters* **28**(12): 2393–2396.

Higurashi A, Nakajima T, Holben BN, Smirnov A, Frouin R, Chatenet B. 2000. A study of global aerosol optical climatology with two-channel AVHRR remote sensing. *Journal of Climate* **13**(12): 2011–2027.

Holben BN, Eck TF, Slutsker I, Tanré D, Buis JP, Setzer A, Vermote E, Reagan JA, Kaufman YJ, Nakajima T, Lavenu F, Jankowiak I, Smirnov A. 1998. AERONET – A federated instrument network and data archive for aerosol characterization. *Remote Sensing of Environment* **66**(1): 1–16.

Holben BN, Tanré D, Smirnov A, Eck TF, Slutsker I, Abuhassan N, Newcomb WW, Schafer JS, Chatenet B, Lavenu F, Kaufman YJ, Vande Castle J, Setzer A, Markham B, Clark D, Frouin R, Halthore R, Karnieli A, O'Neill NT, Pietras C, Pinker RT, Voss K, Zibordi G. 2001. An emerging ground-based aerosol climatology: aerosol optical depth from AERONET. *Journal of Geophysical Research* **106**(D11): 12067–12097.

Holden NM, Brereton AJ. 2004. Definition of agroclimatic regions in Ireland using hydro-thermal and crop yield data. *Agricultural and Forest Meteorology* **122**(3–4): 175–191.

Hsu NC, Herman JR, Torres O, Holben BN, Tanré D, Eck TF, Smirnov A, Chatenet B, Lavenu F. 1999. Comparisons of the TOMS aerosol index with sun-photometer aerosol optical thickness: results and applications. *Journal of Geophysical Research* **104**(D6): 6269–6279.

Im J-S, Saxena VK, Wenny BN. 2001a. Temporal trends of black carbon concentrations and regional climate forcing in the southeastern United States. *Atmospheric Environment* **35**(19): 3293–3302.

Im J-S, Saxena VK, Wenny BN. 2001b. An assessment of hygroscopic growth factors for aerosols in the surface boundary layer for computing direct radiative forcing. *Journal of Geophysical Research* **106**(D17): 20213–20224.

Ingold T, Mätzler C, Kämpfer N. 2001. Aerosol optical depth measurements by means of a Sun photometer network in Switzerland. *Journal of Geophysical Research* **106**(D21): 27537–27554.

IPCC. 2001. *Climate Change 2001: The Scientific Basis. Contribution of Working Group I to the Third Assessment Report of the Intergovernmental Panel on Climate Change*, Houghton JT, Ding Y, Griggs DJ, Noguer M, van der Linden PJ, Dai X, Maskell K, Johnson CA (eds). Cambridge University Press: Cambridge, United Kingdom, New York, 881.

Jacovides CP, Timbios FS, Giannourakos GP, Pashiardis S, Stefanou L. 1996. Recent measurements of broad-band turbidity parameters in the island of Cyprus. *Atmospheric Environment* **30**(20): 3391–3396.

Kalkstein LS, Corrigan P. 1986. A synoptic climatological approach for geographic analysis: assessment of sulfur dioxide concentrations. *Annals of the Association of American Geographers* **76**(3): 381–395.

Kalkstein LS, Webber SR. 1991. A detailed evaluation of scenes air quality data in northern Arizona using a three-dimensional synoptic approach. *Publications in Climatology* **43**(1): 1–98.

Kambezidis HD, Katevatis EM, Petrakis M, Lykoudis S, Asimakopoulos DN. 1998. Estimation of the Linke and Unsworth-Monteith turbidity factors in the visible spectrum: application for Athens, Greece. *Solar Energy* **62**(1): 39–50.

Kay M, Box M. 2000. Radiative effects of absorbing aerosols and the impact of water vapor. *Journal of Geophysical Research* **105**(D10): 12221–12234.

Knapp KR, Vonder Haar TH, Kaufman YJ. 2002. Aerosol optical depth retrieval from GOES-8: Uncertainty study and retrieval validation over South America. *Journal of Geophysical Research* **107**(D7): 4055, DOI: 10.1029/2001JD000505.

Kotchenruther RA, Hobbs PV, Hegg DA. 1999. Humidification factors for atmospheric aerosols off the mid-Atlantic coast of the United States. *Journal of Geophysical Research* **104**(D2): 2239–2251.

Leathers DJ, Mote TL, Grundstein AJ, Robinson DA, Felter K, Conrad K, Sedywitz L. 2002. Associations between continental-scale snow cover anomalies and air mass frequencies across eastern North America. *International Journal of Climatology* **22**(12): 1473–1494.

Lohmann U, Feichter J, Penner J, Leaitch R. 2000. Indirect effect of sulfate and carbonaceous aerosols: a mechanistic treatment. *Journal of Geophysical Research* **105**(D10): 12193–12206.

Malm WC, Day DE. 2001. Estimates of aerosol species scattering characteristics as a function of relative humidity. *Atmospheric Environment* **35**(16): 2845–2860.

Maring H, Savoie DL, Izaguirre MA, McCormick C, Arimoto R, Prospero JM, Pilinis C. 2000. Aerosol physical and optical properties and their relationship to aerosol composition in the free troposphere at Izana, Tenerife, Canary Islands, during July 1995. *Journal of Geophysical Research* **105**(D11): 14677–14700.

Pedrós R, Utrillas MP, Martinez-Lozano JA, Tena F. 1999. Values of broad band turbidity coefficients in a Mediterranean coastal site. *Solar Energy* **66**(1): 11–20.

Penner JE, Andreae M, Annegarn H, Barrie L, Feichter F, Hegg D, Jayaraman A, Leaitch R, Murphy D, Nganga J, Pitari G. 2001. Aerosols, their direct and indirect effects. In *Climate Change 2001: The Scientific Basis. Contribution of Working Group I to the Third Assessment Report of the Intergovernmental Panel on Climate Change*, Houghton JT, Ding Y, Griggs DJ, Noguer M, van der Linden PJ, Dai X, Maskell K, Johnson CA (eds.) Cambridge University Press: Cambridge, United Kingdom, New York; 289–348.

Peterson JT, Flowers EC. 1977. Interactions between air pollution and solar radiation. *Solar Energy* **19**(1): 23–32.

Peterson JT, Flowers EC, Berri GJ, Reynolds CL, Rudisill JH. 1981. Atmospheric turbidity over central North Carolina. *Journal of Applied Meteorology* **20**(3): 229–241.

Pilinis C, Pandis SN, Seinfeld JH. 1995. Sensitivity of direct climate forcing by atmospheric aerosols to aerosol size and composition. *Journal of Geophysical Research* **100**(D9): 18739–18754.

Pinker RT, Ferrare RA, Karnieli A, Aro TO, Kaufman YJ, Zangvil A. 1997. Aerosol optical depths in a semiarid region. *Journal of Geophysical Research* **102**(D10): 11123–11137.

Power HC. 2003. The geography and climatology of aerosols. *Progress in Physical Geography* **27**(4): 502–547.

Power HC, Willmott CJ. 2001. Seasonal and interannual variability in atmospheric turbidity over South Africa. *International Journal of Climatology* **21**(5): 579–591.

Power HC, Goyal A. 2003. Comparison of aerosol and climate variability over Germany and South Africa. *International Journal of Climatology* **23**(8): 921–941.

Ramaswamy V, Boucher O, Haigh J, Hauglustaine D, Haywood J, Myhre G, Nakajima T, Shi GY, Solomon S. 2001. Radiative forcing of climate change. In *Climate Change 2001: The Scientific Basis. Contribution of Working Group I to the Third Assessment Report of the Intergovernmental Panel on Climate Change*, Houghton JT, Ding Y, Griggs DJ, Noguer M, van der Linden PJ, Dai X, Maskell K, Johnson CA (eds.) Cambridge University Press: Cambridge, United Kingdom, New York, 349–416.

Rogerson PA. 2001. *Statistical Methods for Geography*. Sage Publications: London, 236.

Schwartz MD. 1991. An integrated approach to air mass classification in the north central United States. *Professional Geographer* **43**(1): 77–91.

Sheridan SC, Kalkstein LS, Scott JM. 2000. An evaluation of the variability of air mass character between urban and rural areas. In *Biometeorology and Urban Climatology at the Turn of the Millennium*. World Meteorological Organization: Geneva, 487–490.

Sheridan SC. 2002. The redevelopment of a weather-type classification scheme for North America. *International Journal of Climatology* **22**(1): 51–68.

Sheridan SC, Dolney TJ. 2003. Heat, mortality, and level of urbanization: Measuring vulnerability across Ohio, USA. *Climate Research* **24**(3): 255–265.

Shettle EP, Anderson S. 1995. New visible and near IR ozone absorption cross-sections for MODTRAN. In *Proceedings of the 17th Annual Conference on Atmospheric Transmission Models, 8–9 June 1994* Anderson GP, Pickard RH, Chetwynd JH (eds.), 335–345, Publ. PL-TR-95-2060. Geophysics Directorate of the Phillips Laboratory at Hanscom Air Force Base Massachusetts, USA.

Smirnov A, Royer A, O'Neill NT, Tarussov A. 1994. A study of the link between synoptic air mass type and atmospheric optical parameters. *Journal of Geophysical Research* **99**(D10): 20967–20982.

Smirnov A, Villevalde Y, O'Neill NT, Royer A, Tarussov A. 1995. Aerosol optical depth over the oceans: analysis in terms of synoptic air mass types. *Journal of Geophysical Research* **100**(D8): 16639–16650.

Smirnov A, O'Neill NT, Royer A, Tarussov A, McArthur B. 1996. Aerosol optical depth over Canada and the link with synoptic air mass types. *Journal of Geophysical Research* **101**(D14): 19299–19318.

Smirnov A, Holben BN, Dubovik O, O'Neill NT, Remer LA, Eck TF, Slutsker I, Savoie D. 2000. Measurement of atmospheric optical parameters on U.S. Atlantic coast sites, ships, and Bermuda during TARFOX. *Journal of Geophysical Research* **105**(D8): 9887–9901.

Smirnov A, Holben BN, Kaufman YJ, Dubovik O, Eck TF, Slutsker I, Pietras C, Halthore RN. 2002. Optical properties of atmospheric aerosol in maritime environments. *Journal of the Atmospheric Sciences* **59**(3): 501–523.

Treffeisen R, Herber A, Strom J, Shiobara M, Yamagata TY, Holmen K, Kriews M, Schrems O. 2004. Interpretation of Arctic aerosol properties using cluster analysis applied to observations in the Svalbard area. *Tellus Series B-Chemical and Physical Meteorology* **56**(5): 457–476.

United States Environmental Protection Agency. 2004. *The Particle Pollution Report: Current Understanding of Air Quality and Emissions Through 2003*, EPA Publication No. 454-R-04-002, U.S. EPA Office of Air Quality Planning and Standards. Research Triangle Park, North Carolina, USA.

Van Heuklon TK. 1979. Estimating atmospheric ozone for solar radiation models. *Solar Energy* **22**(1): 63–68.

von Hoyningen-Huene W, Wenzel K, Schienbein S. 1999. Radiative properties of desert dust and its effect on radiative balance. *Journal of Aerosol Science* **30**(4): 489–502.

Wenny BN, Schafer JS, DeLuisi JJ, Saxena VK, Barnard WF, Petropavlovskikh IV, Vergamini AJ. 1998. A study of regional aerosol radiative properties and effects on ultraviolet-B radiation. *Journal of Geophysical Research* **103**(D14): 17083–17097.

Yarnal B. 1993. *Synoptic Climatology in Environmental Analysis*. Belhaven Press: London, 192.

Yu S, Zender CS, Saxena VK. 2001. Direct radiative forcing and atmospheric absorption by boundary layer aerosols in the southeastern US: model estimates on the basis of new observations. *Atmospheric Environment* **35**(23): 3967–3977.

Yu S, Saxena VK, Wenny BN, DeLuisi JJ, Yue GK, Petropavlovskikh IV. 2000. A study of the aerosol radiative properties needed to compute direct aerosol forcing in the southeastern United States. *Journal of Geophysical Research* **105**(D20): 24739–24749.

Zhang J, Christopher SA, Holben BN. 2001. Intercomparison of smoke aerosol optical thickness derived from GOES 8 imager and ground-based sun photometers. *Journal of Geophysical Research* **106**(D7): 7387–7397.

